# Instability of the Gravitational N-Body Problem in the Large-N Limit

Marc Hemsendorf and David Merritt

Department of Physics and Astronomy, Rutgers University

# ABSTRACT

We use a systolic N-body algorithm to evaluate the linear stability of the gravitational N-body problem for N up to  $0.6 \times 10^5$ , roughly two orders of magnitude greater than in previous experiments. For the first time, a clear N-dependence of the perturbation growth rate is seen,  $\mu_e \sim \ln N$ . The *e*-folding time for  $N = 10^5$ is roughly 1/20 of a crossing time.

## 1. Introduction

Miller (1964) first noted the remarkable sensitivity of the gravitational N-body problem to small changes in the initial conditions. Errors or perturbations in the coordinates or velocities of one or more stars grow roughly exponentially, with an *e*-folding time that is of order the crossing time and that depends only weakly on the number of particles. The implication, verified in a number of subsequent studies (Lecar 1968; Hayli 1970), is that N-body integrations are not reproducible over time scales that exceed a few crossing times. The instability is somewhat reduced when the Newtonian force law is modified by a cutoff (Standish 1968), indicating that it is driven by close encounters.

Of interest is the behavior of the instability in the limit of large N. It is commonly assumed that the N-body equations of motion go over to the collisionless Boltzmann equation as  $N \to \infty$  (Binney & Tremaine 1987). This would imply, for instance, that a particle trajectory which is integrable in a smooth potential should exhibit increasingly regular behavior as the number of point masses used to represent the smooth potential becomes large. On the other hand, if the growth rate of small perturbations remains substantial even for large N, there would be an important sense in which the collisionless Boltzmann equation does not correctly describe the behavior of N-body systems.

In fact there are indications that the instability growth rate remains constant or even increases with N (Kandrup & Smith 1991; Heggie 1991; Goodman, Heggie & Hut 1993), although this result is uncertain since numerical experiments have so far been limited to  $N \lesssim 500$ . Here we describe the application of a new, "systolic" N-body algorithm to this problem, which allows us to treat systems with N as large as  $10^5$ . We observe for the first time a clear N-dependence of the instability: the growth rate increases approximately as  $\ln N$ . Our methods and results are described in §2 and §3, and the implications for galactic dynamics are discussed in §4.

# 2. Method

Following Miller (1971), we integrated the coupled N-body and variational equations:

$$\ddot{\mathbf{x}}_i = -Gm \sum_{j=1}^N \frac{\mathbf{x}_i - \mathbf{x}_j}{|\mathbf{x}_i - \mathbf{x}_j|^3}$$
(1)

$$\ddot{\mathbf{X}}_{i} = -Gm \sum_{j=1}^{N} \left[ (\mathbf{X}_{i} - \mathbf{X}_{j}) - 3 \frac{(\mathbf{X}_{i} - \mathbf{X}_{j}) \cdot (\mathbf{x}_{i} - \mathbf{x}_{j})}{|\mathbf{x}_{i} - \mathbf{x}_{j}|^{2}} (\mathbf{x}_{i} - \mathbf{x}_{j}) \right] \times \frac{1}{|\mathbf{x}_{i} - \mathbf{x}_{j}|^{3}}.$$
 (2)

Here  $\mathbf{x}_i$  are the configuration-space coordinates of the *i*th particle and  $\mathbf{X}_i$  are the components of its variational vector. The masses *m* are assumed equal. The variational equations represent the time development of the infinitesimal distance between two neighboring *N*body systems.

Equations (1) and (2) were integrated using the systolic N-body algorithm described by Dorband, Hemsendorf & Merritt (2002). This algorithm implements the fourth-order Hermite integration as described by Makino & Aarseth (1992). We adopted their formula for computing the time step of particle i,

$$\Delta t_i = \sqrt{\eta \frac{|\mathbf{a}_i(t_1)||\mathbf{a}_i^{(2)}(t_1)| + |\dot{\mathbf{a}}_i(t_1)|^2}{|\dot{\mathbf{a}}_i(t_1)||\mathbf{a}_i^{(3)}(t_1)| + |\mathbf{a}_i^{(2)}(t_1)|^2}}.$$
(3)

Here **a** is the acceleration  $\ddot{\mathbf{x}}$ , superscripts denote the order of the time derivative,  $t_1$  is the system time, and  $\eta$  is a dimensionless constant; we set  $\eta = 0.02$ . The same time step was used to integrate both the N-body and variational equations. The systolic algorithm distributes the particles equally among p processors and computes forces by systematically shifting the particle coordinates between processors in a ring. A single processor was used for small particle numbers while 64 processors were used for the largest-N runs (Table 1). The multi-processor runs were carried out using the Cray T3E computer at the Höchstleistungsrechenzentrum in Stuttgart.

Initial conditions were generated randomly from the isotropic Plummer model, whose

density and potential satisfy

$$\rho(r) = \frac{3GM}{4\pi} \frac{b^2}{\left(r^2 + b^2\right)^{5/2}}, \qquad \Phi(r) = -\frac{GM}{\sqrt{r^2 + b^2}}.$$
(4)

We adopted standard N-body units (Heggie & Mathieu 1986) such that G = M = 1, E = -1/4, giving a scale factor  $b = 3\pi/16$ . We defined the crossing time  $t_{cr}$  as R/V, with  $R \equiv -GM^2/2E$  and  $V^2 \equiv -2E/M$ ; in these units,  $t_{cr} = 2\sqrt{2}$ . The variational vectors **X** and **V** were assigned an initial amplitude of  $10^{-30}$  for each particle with randomly chosen directions.

The parameters of the runs are listed in Table 1. Each run was continued until a time of 20, or roughly 7 crossing times. This time is short enough that two-body relaxation should not be important even for the smallest N, and long enough to show a clearly exponential growth of the solutions of the variational equations.

We focussed on the amplitudes of the Cartesian components of the variational vectors,  $\mathbf{X}_i = (X_i, Y_i, Z_i)$ , since the variational velocities tend to exhibit spikes in their time dependence (Miller 1964). We examined three choices for the amplitude  $\Delta$  of the separation:

- 1.  $\Delta_m$ , the maximum over *i* of the  $|\mathbf{X}_i|$ .
- 2.  $\Delta_a$ , the arithmetic mean of the  $|\mathbf{X}_i|$ .
- 3.  $\Delta_g$ , the geometric mean of the  $|\mathbf{X}_i|$ .

The instability growth rate  $\mu_e$  was defined as

$$\mu_e = \frac{\ln \Delta(t_2) - \ln \Delta(t_1)}{t_2 - t_1}.$$
(5)

Except in the case of small  $N, N \leq 1024$ , growth in the variation was found to be nearly exponential and hence the computed values of  $\mu_e$  depended only weakly on  $t_2$  and  $t_1$ . We chose  $t_1 = 1$  and  $t_2 = 20$ .

#### 3. Results

The three amplitudes  $\Delta$  defined above were found to be very similar in most of the integrations, as shown in Figure 1 for the 10 runs with N = 32768. In what follows we adopt  $\Delta \equiv \Delta_g$ , the geometric mean.

Figure 2a shows  $t_e \equiv \mu_e^{-1}$  for each of the runs. The mean value of the *e*-folding time and its uncertainty are plotted in Figure 2b; the latter was defined as the standard error of the mean, or  $n^{-1/2}$  times the standard deviation, with *n* the number of distinct *N*-body integrations. For the first time, a clear *N*-dependence can be seen, in the sense that the average value of  $t_e$  declines with increasing *N*: large-*N* systems are more unstable than small-*N* systems.

A number of predictions have been made for the large-N dependence of the *e*-folding time. Gurzadyan & Savvidy (1986) estimated  $t_e \sim N^{1/3}t_{cr}$  based on a geometrical approach. This prediction is clearly inconsistent with Figure 2; Gurzadyan & Savvidy's approach was criticized already by Heggie (1991) and Goodman, Heggie & Hut (1993) due to its improper treatment of close encounters. The latter authors argued that  $t_e/t_{cr} \sim 1/\ln N$  or  $\sim 1/\ln(\ln N)$ ; the weaker dependence would only hold after a time long enough that the perturbation from one star was able to propagate throughout the system.

We tested these predictions against the N-body data. Figure 3 shows fits of two functional forms to the average growth rates:

$$\mu_e = a + b \ln N, \tag{6}$$

$$\mu_e = c + d\ln(\ln N). \tag{7}$$

Since any such relation is expected to be valid only in the limit of large N, we restricted the fits to  $N \ge 1024$ ; furthermore the integrations with smaller N have substantially larger error bars on  $\mu_e$ . The best-fit parameters are given in Table 2. We used a standard least-squares routine that accounts for errors in the dependent variable  $(\mu_e)$ ; in the case of the data point with N = 65536, for which there was only one integration, the uncertainty in  $\mu_e$  was assumed to be the same as in the integration with N = 32768.

The reduced  $\chi^2$  is close to 2 for both model fits; while a constant  $\mu_e t_{cr}$  can clearly be ruled out, we can not distinguish between a  $\ln N$  or  $\ln(\ln N)$  dependence. Expressed in terms of  $t_e$  and  $t_{cr}$ , the best-fit relations are

$$t_e/t_{cr} \approx \frac{1.01}{\ln(1.45 \times 10^3 N)},$$
 (8)

$$t_e/t_{cr} \approx \frac{0.116}{\ln(0.73\ln N)}$$
 (9)

Distinguishing between these two functional forms, or other similar ones, would clearly be very difficult; even for  $N = 10^6$ , the two relations predict values of  $t_e$  that differ only by ~ 5%. Equation (9) is close to a relation suggested by Hut & Heggie (2001), except for a factor of ~ 2 difference in the normalization.

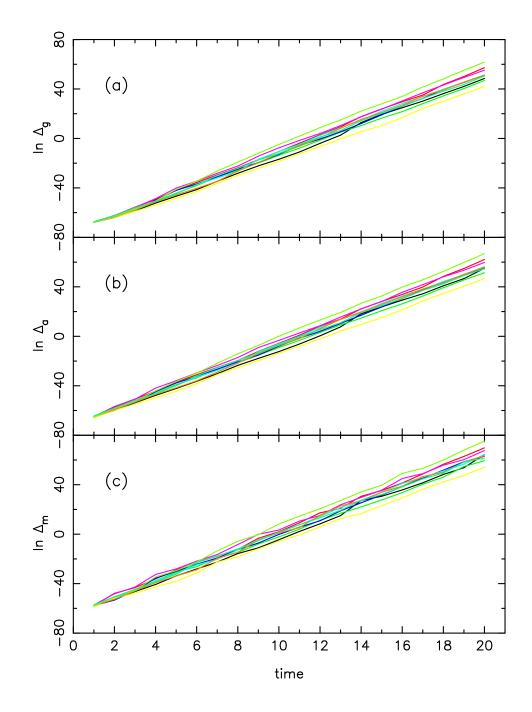


Fig. 1.— Growth of the variation in the spatial coordinate for 10 Plummer-model integrations with N = 32768. (a)  $\Delta_g$ , the geometric mean of the variations. (b)  $\Delta_a$ , the arithmetic mean of the variations. (c)  $\Delta_m$ , the maximum variation.

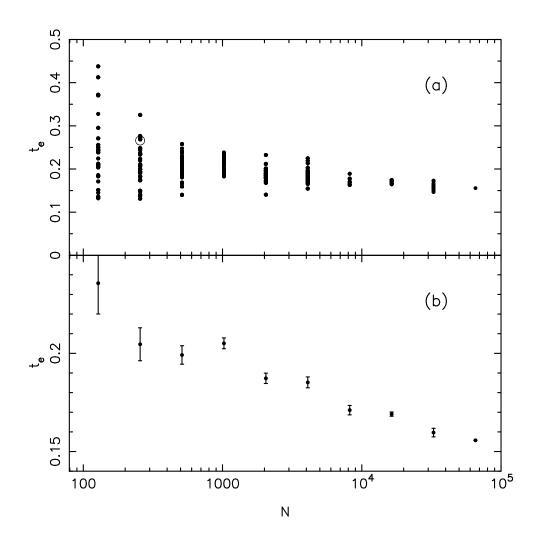


Fig. 2.— Exponentiation times for the *N*-body integrations. (a)  $t_e$  for each of the runs. The open circle is the mean value of  $t_e$  quoted by Goodman et al. (1993) from seven integrations of an N=256 Plummer model. (b) Mean values of  $t_e$  for each *N*. Error bars represent the standard error of the mean.

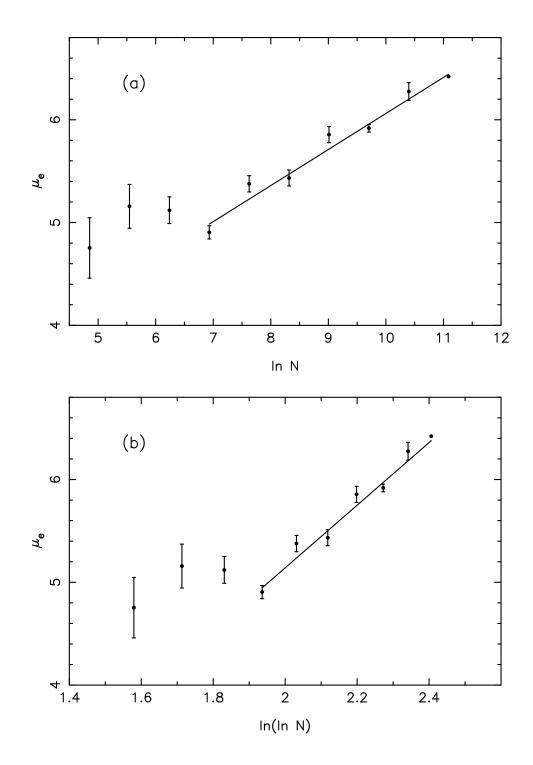


Fig. 3.— Fits of the *N*-body growth rates to two functional forms,  $\mu_e \propto \ln N$  and  $\mu_e \propto \ln(\ln N)$ . Fitting parameters are given in Table 2.

## 4. Discussion

In statistical mechanics, instability of trajectories is often linked to mixing, the tendency of an initially localized ensemble of phase points to uniformly fill their accessible phase-space region. For instance, in the hard-sphere gas, the relaxation time is closely correlated with the Liapunov exponents describing the degree of chaos of individual trajectories (Sinai 1970). This correspondence has led a number of authors to suggest that the generic instability of gravitational N-body systems should imply evolution to a relaxed state on a time scale much shorter than the standard two-body relaxation time (Gurzadyan & Savvidy 1986; Pucacco 1992).

However there are dynamical systems in which mixing occurs on a much longer time scale than that associated with divergence of nearby trajectories (e.g. Merritt & Valluri 1996). Gravitational N-body systems appear to be in this class. For instance, single orbits integrated in "frozen" N-body potentials behave more and more like their smooth-potential counterparts as N is increased, even though their Liapunov exponents remain large (Valluri & Merritt 2000; Kandrup & Sideris 2001). Such experiments suggest that the collisionless Boltzmann equation may be a good predictor of the macroscopic dynamics of large-N systems even if it does not reproduce the small-scale chaos measured here.

This work was supported by NSF grant 00-71099 and by NASA grants NAG5-6037 and NAG5-9046 to DM. We thank J. Goodman and D. Heggie for useful conversations. We are grateful to the Höchstleistungsrechenzentrum in Stuttgart for their generous allocation of computer time.

#### REFERENCES

Binney, J. & Tremaine, S. 1987, Galactic Dynamics (Princeton: Princeton University Press)

- Dorband, N., Hemsendorf, M. & Merritt, D. 2001, J. Comp. Phys., in press (astroph/0112092)
- Goodman, J., Heggie, D. C., & Hut, P. 1993, ApJ, 415, 715
- Gurzadyan, V. & Savvidy, G. 1986, A&A, 160, 203
- Hayli, A. 1970, A&A, 7, 249
- Heggie, D. C. 1991, in Predictability, Stability, and Chaos in N-Body Dynamical Systems, ed. A. E. Roy (New York: Plenum Press), p. 47

- Heggie, D. C. & Mathieu, R. D. 1986, in The Use of Supercomputers in Stellar Dynamics, ed. P. Hut & S. L. W. McMillan (Berlin: Springer), 233
- Hut, P. & Heggie, D. C. 2001, astro-ph/0111015
- Kandrup, H. E. & Sideris, I. V. 2001, Phys. Rev. E, 64, 6209
- Kandrup, H. E. & Smith, H. 1991, ApJ, 374, 255
- Lecar, M. 1968, Bull. Astron. 3, 91
- Makino, J. & Aarseth, S. J. 1992, PASJ, 44, 141
- Merritt, D. & Valluri, M. 1996, ApJ, 471, 82
- Miller, R. H. 1964, ApJ, 140, 250
- Miller, R. H. 1971, J. Comput. Phys., 8, 449
- Pucacco, G. 1992, A&A, 259, 473
- Sinai, Ya. G. 1970, Russian Mathematical Reviews 25, 137
- Spitzer, L. 1987, Dynamical Evolution of Globular Clusters (Princeton: Princeton University Press)
- Standish, E. M. 1968, PhD thesis, Yale University
- Valluri, M. & Merritt, D. 2000, in The Chaotic Universe, eds. V. G. Gurzadyan & R. Ruffini (Singapore: World Scientific), p. 229.

This preprint was prepared with the AAS  ${\rm IAT}_{\rm E} {\rm X}$  macros v5.0.

	N	n	p	$\langle t_e \rangle$	$\sigma_{t_e}$	$\langle \mu_e \rangle$	$\sigma_{\mu_e}$
-	128	35	1	0.236	0.016	4.75	0.29
	256	35	1	0.205	0.008	5.16	0.21
	512	35	1	0.199	0.005	5.12	0.13
	1024	35	1	0.205	0.003	4.91	0.064
	2048	35	1	0.187	0.003	5.38	0.079
	4096	35	1	0.185	0.003	5.43	0.078
	8192	10	1	0.171	0.002	5.86	0.078
	16384	10	64	0.169	0.001	5.92	0.038
	32768	10	64	0.160	0.002	6.28	0.086
	65536	1	64	0.156		6.42	—

Table 1: Parameters of the *N*-body runs. *N* is the particle number; *n* is the number of distinct integrations; *p* is the number of processors used;  $\langle t_e \rangle$  and  $\sigma_{t_e}$  are the mean *e*-folding time and its error;  $\langle \mu_e \rangle$  and  $\sigma_{\mu_e}$  are the mean *e*-folding rate and its error.

X, Y Variables	a	b	$\chi^2_r$
$\ln N,  \mu_e$	$2.55\pm0.18$	$0.350\pm0.02$	2.1
$\ln(\ln N), \mu_e$	$-0.954\pm0.37$	$3.05\pm0.17$	2.0

Table 2: Results of the linear regression fits, Y = a + bX.